



Onset timing of left-lateral movement along the Ailao Shan–Red River Shear Zone: $^{40}\text{Ar}/^{39}\text{Ar}$ dating constraint from the Nam Dinh Area, northeastern Vietnam

Pei-Ling Wang^{a,*}, Ching-Hua Lo^b, Sun-Lin Chung^b, Tung-Yi Lee^c, Ching-Ying Lan^a,
Trang Van Thang^d

^a*Institute of Earth Sciences, Academia Sinica, Taipei, Taiwan*

^b*Department of Geology, National Taiwan University, Taipei, Taiwan*

^c*Department of Earth Sciences, National Taiwan Normal University, Taipei, Taiwan*

^d*Institute of Geological Sciences, National Center for Natural Sciences and Technology, Hanoi, Viet Nam*

Received 20 December 1998; accepted 16 June 1999

Abstract

Left-lateral motion along the Ailao Shan–Red River (ASRR) Shear Zone has been widely advocated to be the result of the collision between the Indian and Eurasian plates and to account for sea-floor spreading in the South China Sea. Our new $^{40}\text{Ar}/^{39}\text{Ar}$ data on the south-easternmost outcrop of the Day Nui Con Voi metamorphic massif, northern Vietnam, suggest that the exhumation of metamorphic massifs by shearing along the ASRR zone began ~ 27 Ma and lasted until ~ 22 Ma. A perfect correlation between location and cooling path for the samples along the shear zone suggests that the transtensional deformation may have propagated northwestward at a rate of ~ 6 cm y^{-1} . Such a good correlation also indicates that the onset of the left-lateral movement of the shear zone may have occurred later than ~ 27.5 Ma. This conclusion is consistent with our previous interpretation that collision-induced southeastward extrusion of Indochina along the ASRR Shear Zone postdates the opening of the South China Sea, and that extrusion tectonics in SE China may not be responsible for the opening of the South China Sea. © 2000 Elsevier Science Ltd. All rights reserved.

1. Introduction

Strike-slip motion along the Ailao Shan–Red River (ASRR) Shear Zone has been widely regarded as compensating the convergence between India and Eurasia (Fig. 1(a)). On the basis of laboratory models and geological evidence, Tapponnier et al. (1982, 1986) and Peltzer and Tapponnier (1988) proposed a collision–extrusion model to explain the tectonic consequences of the India–Eurasia collision during the Tertiary. In this model, the eastward extrusion of Indochina along the ASRR Shear Zone not only takes up a substantial amount of the convergence between India and Eurasia,

but is also responsible for the opening of the South China Sea. This interpretation seemed to have been supported by comparison of the offset along the shear zone with the history of seafloor spreading in the South China Sea with regard to distance and rate. For instance, Briais et al. (1993) and Leloup et al. (1995) indicated that the offset derived from the fit of magnetic isochrons on the South China Sea floor was compatible with the sinistral displacement estimated by detailed correlation of geological markers along the ASRR Shear Zone. The propagation rate of left-lateral shearing along the ASRR zone, estimated from thermochronological data, was in good agreement with the estimated spreading rate of the South China Sea as well (Harrison et al., 1996).

Based on the good correlation of two magmatic

* Corresponding author.

E-mail address: plwang@earth.sinica.tw (P.L. Wang).

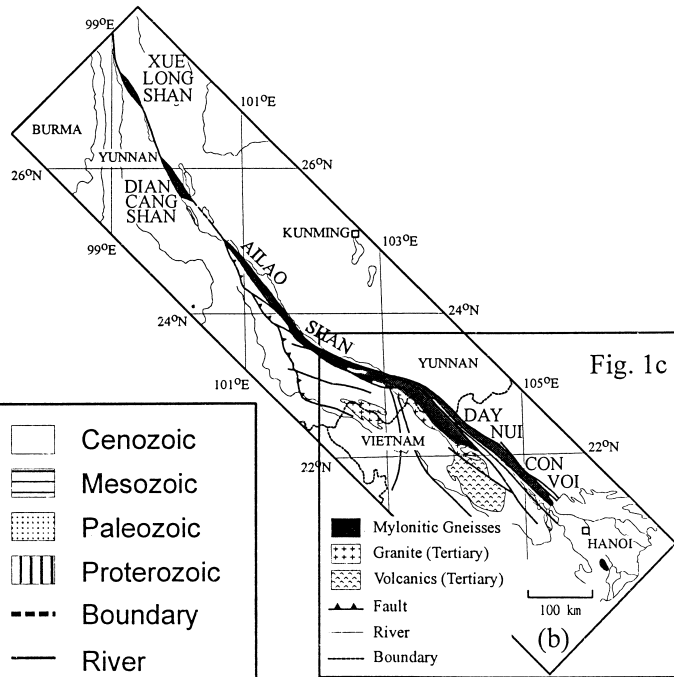
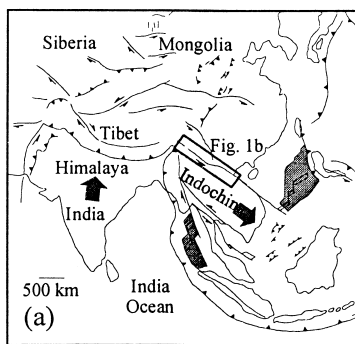
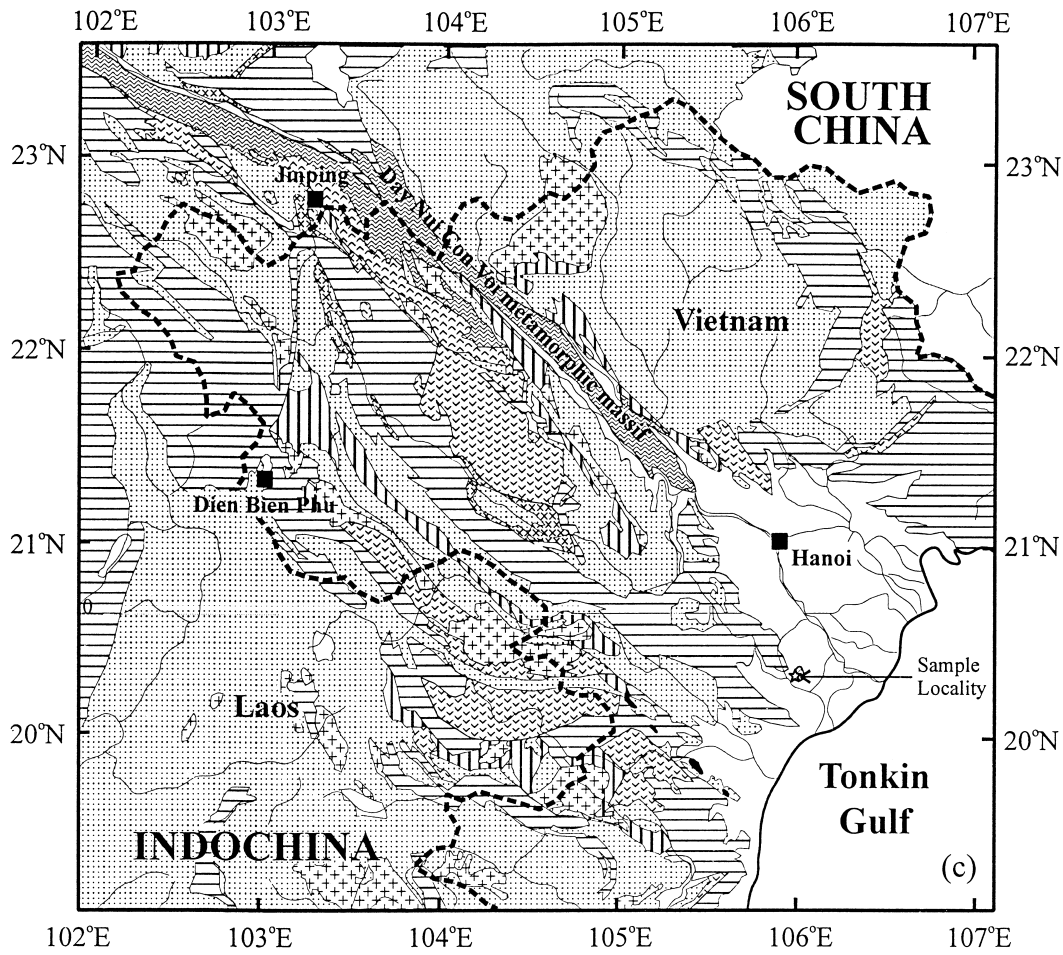


Fig. 1. (a) Tectonic sketch map of SE Asia, modified from Tapponnier et al. (1982); (b) distribution of metamorphic complexes along the ASRR shear zone, modified from Leloup et al. (1995); (c) simplified geologic map of northern Vietnam, modified from Geological Survey of Vietnam (1988). The star indicates the sample locality of this study.

suites on either side of the ASRR Shear Zone in SW China and northern Vietnam, Chung et al. (1997) suggested the existence of a 600 km left-lateral displacement, younger than 30 Ma, along the ASRR Shear Zone. This observation has been confirmed further by thermochronological results, that indicate a rapid change of cooling rates during the late Oligocene–Early Miocene (27–17 Ma) for the shear zone in southern Yunnan and northern Vietnam (Harrison et al., 1996; Wang et al., 1998). This would imply that the initiation of movement along the ASRR Shear Zone actually postdated the initiation of seafloor spreading of the South China Sea which started from magnetic anomaly 11 (Taylor and Hayes, 1983; Briais et al., 1993), corresponding to 30 Ma, according to the new geomagnetic polarity timescale of Cande and Kent (1995). Moreover, previous seismic studies at the termination of the Red River Fault also demonstrated that the opening of the South China Sea was not linked to the Red River Fault but was controlled by right-lateral shearing along the eastern coast of Vietnam (Rangin et al., 1995; Roques et al., 1997). In this case, extrusion tectonics may not be responsible for the opening of the South China Sea, and the mechanisms responsible for the opening of the South China Sea and the development of the ASRR Shear Zone would still remain to be ascertained. In order to further tackle this problem, the age of the onset of the activity along the ASRR Shear Zone needs to be addressed in greater detail.

Systematic thermochronological analyses of the metamorphic massifs within the ASRR Shear Zone indicate that the exhumation and/or deformation front was propagating from the southeast to the northwest at a rate of 4 to 5 centimeters per year (Harrison et al., 1996; Wang et al., 1998). Accordingly, the earliest record of left-lateral motion along the shear zone should be observed at the southernmost part of the Day Nui Con Voi metamorphic massif in northeastern Vietnam. This paper presents the results of a ^{40}Ar – ^{39}Ar thermochronological study for the southernmost outcrop of the Day Nui Con Voi metamorphic massif, located in the south of Nam Dinh, northeastern Vietnam. It is hoped that the results provide better constraints for the onset timing of the left-lateral movement along the ASRR Shear Zone.

2. Geological setting

The ASRR Shear Zone extends over 1000 km between eastern Tibet and the Tonkin Gulf, and comprises four narrow metamorphic massifs. From NW to SE, these are the Xuelong Shan, the Diancang Shan, the Ailao Shan (in Yunnan) and the Day Nui Con Voi (in Vietnam) (Fig. 1(b)). These massifs consist mainly

of high-grade mylonitic gneisses with amphibolite enclaves, leucogranite, and pegmatite veins. Most of them exhibit well-defined foliation, striking nearly parallel to the trend of the shear zone, with clear markers indicating a left-lateral sense of shearing for ductile deformation along the shear zone, except those in some leucogranite and pegmatite veins (e.g. Leloup et al., 1995).

The Day Nui Con Voi metamorphic massif in northern Vietnam is the southernmost range of the ASRR Shear Zone. It is bounded by NW-trending normal faults and lies adjacent to Neogene–Quaternary basins. Toward the southeast the massif is progressively submerged and covered by Quaternary sediments of the Red River Delta (Fig. 1(c)) (Geological Survey of Vietnam, 1988). Geothermobarometric studies suggest the peak metamorphic conditions to have been $690 \pm 30^\circ\text{C}$ and 0.65 ± 0.15 GPa. Subsequent mylonitization occurred at 480°C and 0.3 GPa (Nam et al., 1998). Previous $^{40}\text{Ar}/^{39}\text{Ar}$ thermochronological results indicate that this massif was exhumed and cooled slowly before 25 Ma, followed by fast cooling and exhumation at around 25–21 Ma (Wang et al., 1998).

3. Samples and analytical methods

Samples for the present geochronological study were collected from an outcrop in the Red River Delta, south of Nam Dinh, northern Vietnam, which is apparently the southeasternmost outcrop of the Day Nui Con Voi metamorphic massif (Fig. 1(c)). The samples include a deformed pegmatitic vein (RR58A), a mylonitic gneiss (RR58B) and migmatites (RR58C and D). In thin section, all samples exhibit a similar mineral assemblage including quartz, K-feldspar, plagioclase, biotite, muscovite, garnet, sillimanite and oxides in variable abundance.

$^{40}\text{Ar}/^{39}\text{Ar}$ step-heating experiments were performed on muscovite, biotite, and K-feldspar extracted from the samples. Mineral separates were obtained by standard procedures with magnetic separation, paper shaking, followed by hand-picking, in order to remove all visible impurities. 250–425 or 425–850 μm size fractions were selected for argon isotopic analyses, depending on the natural grain-size of minerals. Mineral separates, along with neutron flux monitor LP-6 biotite (Odin et al., 1982), were irradiated in the VT-C position of the Tsing-Hua Open-Pool Reactor (THOR) at the Tsing-Hua University for 8 h with a fast neutron flux of $1.566 \times 10^{13} \text{ n (cm}^{-2} \text{ s)}^{-1}$. After irradiation, the samples were degassed with a 30 min heating schedule. The isotopic composition was measured using a Varian-MAT GD150 mass spectrometer at the National Taiwan University. Analytical procedures and data processing are described in detail

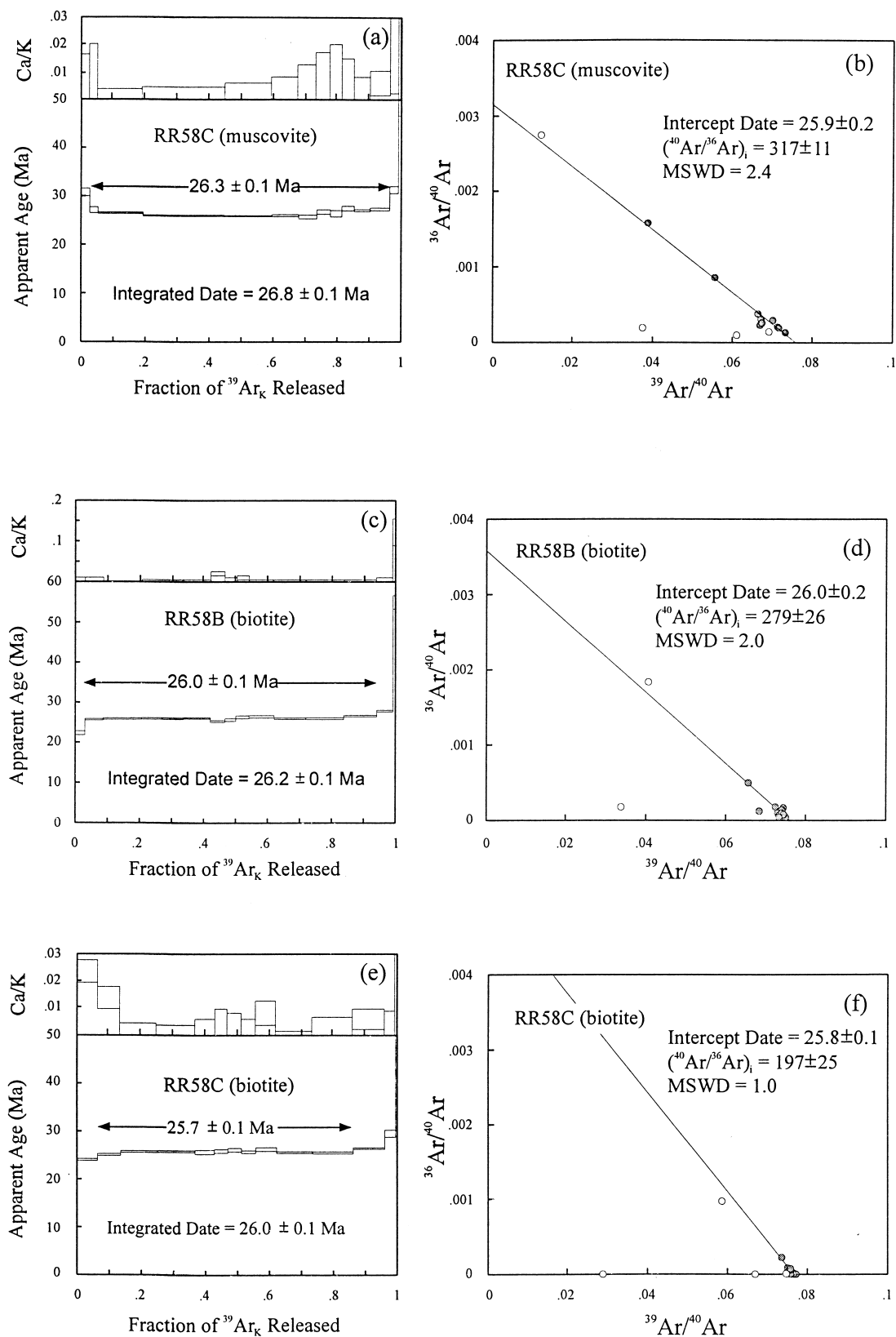


Fig. 2. Age spectra and $^{36}\text{Ar}/^{40}\text{Ar}$ - $^{39}\text{Ar}/^{40}\text{Ar}$ isotope correlation diagrams for micas. The plateau dates are indicated by the arrows in the spectrum plots. The length of steps represents the relative volume of $^{39}\text{Ar}_K$ released, and the height of the open rectangles indicates the 2σ relative uncertainties. In the $^{36}\text{Ar}/^{40}\text{Ar}$ - $^{39}\text{Ar}/^{40}\text{Ar}$ correlation diagrams, the solid lines indicate the results of regression analysis of the data of the plateau steps as shown by solid circles.

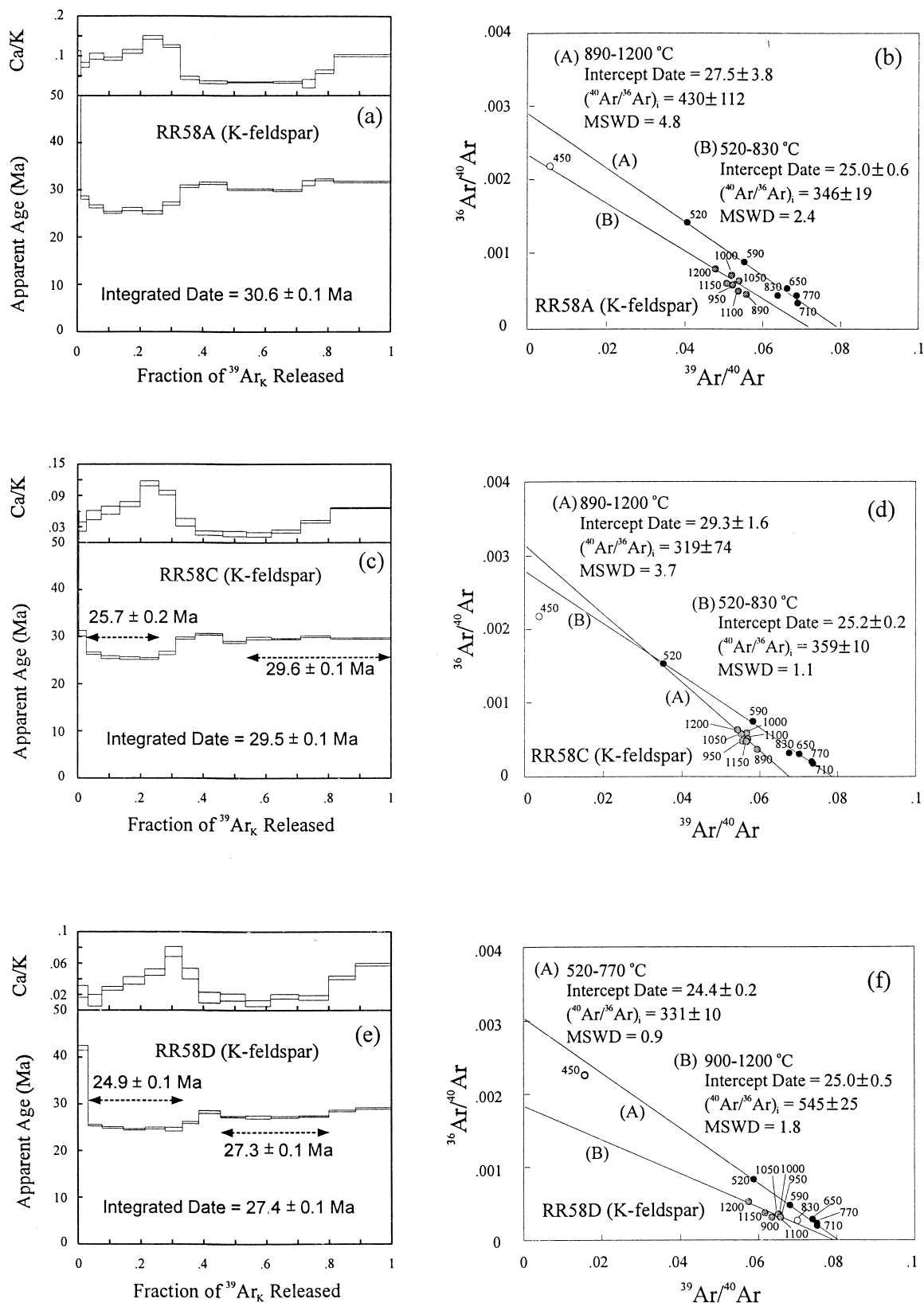


Fig. 3. Age spectra and $^{36}\text{Ar}/^{40}\text{Ar}$ - $^{39}\text{Ar}/^{40}\text{Ar}$ correlation diagrams for K-feldspars. See Fig. 2 and text for details.

by Lo and Lee (1994). After corrections for mass discrimination, system blanks, isotope interference and radiometric decays, the data were plotted as age spectra and $^{36}\text{Ar}/^{40}\text{Ar}$ versus $^{39}\text{Ar}/^{40}\text{Ar}$ isotope correlation diagrams (Figs. 2 and 3). Plateau dates were calculated from the sum of total gas for the continuous steps with dates agreeing with each other to within 2σ . $^{36}\text{Ar}/^{40}\text{Ar}$ versus $^{39}\text{Ar}/^{40}\text{Ar}$ isotope correlation diagrams were plotted to examine the possible components of the gas reservoirs in the minerals. A summary of the $^{40}\text{Ar}/^{39}\text{Ar}$ dating results is given in Table 1. For accurately estimating the closure temperatures, the chemical composition of the biotites were determined by electron probe microanalysis using a JEOL superprobe 8900 at the Institute of Earth Sciences, Academia Sinica. The operating condition was 15 kV acceleration potential and 10 mA beam current.

4. Results

Muscovite from migmatite RR58C yields a flat age spectrum with a well-defined plateau over 90% of cumulative $^{39}\text{Ar}_K$ released, exhibiting a plateau date of 26.3 ± 0.1 Ma (Fig 2(a)). Biotites from RR58B mylonitic gneiss and RR58C migmatite also display fairly flat age spectra with well-defined plateaus over most of the $^{39}\text{Ar}_K$ released ($>80\%$), with plateau dates of 26.0 ± 0.1 Ma and 25.7 ± 0.1 Ma respectively (Figs. 2(c), 2(e)). Intercept dates obtained from least-square regression of data for plateau steps of micas are all highly confident and perfectly consistent with their respective plateau dates (Table 1). $^{40}\text{Ar}/^{36}\text{Ar}$ intercept values generally agree with the atmospheric composition ($^{40}\text{Ar}/^{36}\text{Ar} = 295.5$) (Figs. 2(b), 2(d)), except for biotite in sample RR58C (Fig. 2(f)). The argon isotope composition of RR58C biotite is so radiogenic that it

appears to be difficult to obtain a meaningful regression for the data.

All K-feldspars from the present samples display similar shaped age spectra with an abnormally old date in the first several percent of gas released, followed by relatively young but consistent dates over a flat segment of age spectrum for about 30% of gas released. Then the apparent age increases to another flat segment over the last 60% of gas released (Figs. 3(a), 3(c), 3(e)). In isotope correlation diagrams, the data form two linear arrays for each K-feldspar, comprising the data for the low- and high-temperature steps respectively (Figs. 3(b), 3(d), 3(f)). These two arrays would suggest the presence of at least three gas reservoirs in these samples. Regression of the data from high temperature steps of RR58A K-feldspar yields a higher $^{40}\text{Ar}/^{36}\text{Ar}$ intercept value (424 ± 11) than atmospheric composition (295.5) and a younger intercept date (27.7 ± 0.5 Ma) with respect to its apparent age. Regression for the low temperature steps gives a reasonable $^{40}\text{Ar}/^{36}\text{Ar}$ intercept value (346 ± 19) with an intercept date of 25.0 ± 0.6 Ma, which is indistinguishable from the respective apparent ages (Figs. 3(a), 3(b)). This phenomenon has not been found in RR58C K-feldspar, in which both the $^{40}\text{Ar}/^{36}\text{Ar}$ intercept value and the intercept date are roughly consistent with normal atmospheric composition and their respective values in this K-feldspar (Figs. 3(c), 3(d)). In contrast, least-square regression of the data from high-temperature steps of RR58D K-feldspar yields an abnormal high $^{40}\text{Ar}/^{36}\text{Ar}$ intercept value (545 ± 25) with an intercept date of 25.0 ± 0.5 Ma. The age is generally consistent with the intercept date (24.4 ± 0.2 Ma) and integrated apparent age (24.9 ± 0.1 Ma) for low temperature steps in RR58D K-feldspar (Figs. 3(e), 3(f)). The unusually high $^{40}\text{Ar}/^{36}\text{Ar}$ intercept values would suggest the existence of excess argon in these K-feldspars.

Table 1
Summary of $^{40}\text{Ar}/^{39}\text{Ar}$ dating results in Nam Dinh area^d

Sample	Mineral type ^a	Integrated date (Ma)	Plateau date (Ma)	Intercept date (Ma)	$(^{40}\text{Ar}/^{36}\text{Ar})_i$	MSWD ^b	
RR58A: pegmatite	Kfs	30.6 ± 0.1		25.0 ± 0.3	346 ± 19	2.4	(LT) ^c
				27.7 ± 0.5	424 ± 11	4.4	(HT)
RR58B: gneiss	bt	26.2 ± 0.1	26.0 ± 0.1	26.0 ± 0.2	279 ± 26	2.0	
RR58C: migmatite ^{CG}	ms	26.8 ± 0.1	26.3 ± 0.1	25.9 ± 0.2	317 ± 11	2.4	
	bt	26.0 ± 0.1	25.7 ± 0.1	25.8 ± 0.1	197 ± 25	1.0	
	Kfs	29.5 ± 0.1	25.7 ± 0.2	25.2 ± 0.2	359 ± 10	1.1	(LT)
RR58D: migmatite ^{FG}	Kfs	27.4 ± 0.1	29.6 ± 0.1	29.3 ± 1.6	319 ± 74	3.7	(HT)
			25.0 ± 0.1	24.4 ± 0.2	331 ± 10	0.9	(LT)
			27.3 ± 0.1	25.0 ± 0.9	545 ± 66	1.8	(HT)

^a Kfs: K-feldspar; bt: biotite; ms: muscovite.

^b MSWD: Mean squared weighted deviation.

^c LT: lower-temperature steps; HT: higher temperature steps. CG: coarse-grained; FG: fine-grained.

^d Note: All data errors are shown in 1σ .

5. Thermochronology of the metamorphic massif

The estimated temperature conditions of peak metamorphism in the Day Nui Con Voi massif (~690°C) (Nam et al., 1998) appear to be higher than the generally accepted argon closure temperatures for the minerals analysed in the present study (<550°C, as summarized in McDougall and Harrison, 1988). This suggests that the $^{40}\text{Ar}/^{39}\text{Ar}$ dates obtained for minerals in the Day Nui Con Voi massif would represent the time when the rocks cooled through the argon closure temperatures of the minerals during exhumation. In this case, $^{40}\text{Ar}/^{39}\text{Ar}$ dates, combined with their respective closure temperatures, which can be estimated quantitatively by applying the closure temperature theory of Dodson (1973), would allow to compute the cooling paths for the samples. One of the ways to derive a cooling curve is to date a series of minerals having variable closure temperatures and then to fit a cooling curve through these time-temperature points (McDougall and Harrison, 1988). An alternative way is to fit a cooling curve, using the multiple domain diffusion (MDD) model for the K-feldspar $^{40}\text{Ar}/^{39}\text{Ar}$ age spectrum (Lovera et al., 1991).

According to Dodson (1973), the closure temperature (T_c) is a function of diffusion size (a); activation energy (E); diffusion geometry factor (A); pre-exponential factor of diffusivity (D_0) for the argon diffusion; and cooling rate (dT/dt). It can be formulated as:

$$T_c = \frac{E/R}{\ln \frac{ART_c^2 D_0 / a^2}{E dT/dt}}$$

Accordingly, the closure temperatures for micas in the present study were calculated utilizing the available hydrothermal experimental data on activation energy (E) and pre-exponential factor of argon diffusion (D_0) as given in Table 2. Because argon diffusion in muscovite and biotite appear to follow the cylindrical geometry, $A = 27$ was chosen for the calculations (McDougall and Harrison, 1988). As a first approximation, the mean values of half of the grain sizes were considered

as the size of argon diffusion (a) for minerals. With suitable diffusion parameters, the closure temperatures were calculated for the micas analysed in the present study.

Modelling of the RR58C and RR58D K-feldspar age spectra, assuming a discrete distribution of domain size for argon diffusion, are shown in Figs. 4 and 5. The results provide excellent fits of the Arrhenius versus $\log(r/r_0)$ plots based on eight domains with activation energy of 21.8 kcal mole⁻¹ for RR58C K-feldspar (Figs. 4(b), 4(c)) and four domains with activation energy of 31.8 kcal mole⁻¹ for RR58D K-feldspar (Figs. 5(b), 5(c)). Accordingly, theoretical age spectra were calculated to best fit the age spectra obtained from the experiments, which have been corrected for the possible effects of the excess argon component, derived from their isotope correlation diagrams (Figs. 4(a), 5(a)). The result shows that RR58C K-feldspar cooled very fast at a rate of 170 to 180°C my⁻¹ by 29 Ma. Then the sample seems to be remained isothermally at around 180°C until 25 Ma and cooled rapidly again during a later stage (Fig. 4(d)). Because of the unreliable regression for higher-temperature steps of RR58C K-feldspar (MSWD > 2.5) (Fig. 3(d)), the cooling path above 200°C may not be as reliable as those indicated by low-temperature steps. In contrast, RR58D K-feldspar behaviour is totally different from RR58C K-feldspar in its cooling path, in that it simply cooled quickly at a rate of 140°C my⁻¹ from 27.5 to 24.7 Ma (Fig. 5(d)).

All thermochronological data are summarized in Fig. 6. Excluding the less reliable estimate of the cooling path for RR58C K-feldspar, the general cooling path of the metamorphic rocks in this outcrop can be summarized as starting fast cooling at around 27 to 25 Ma at a rate greater than 100°C my⁻¹. This cooling path is very similar to those obtained by previous studies for samples from areas further northwest of the Day Nui Con Voi metamorphic massif (Nam et al., 1998; Wang et al., 1998), except that the age of the initiation of fast cooling appears to be slightly older (Fig. 7). Nevertheless, the good correlation of the age of fast cooling, the sample location, and the northwesterly progression of the age for fast cooling remain the

Table 2
Argon diffusion parameters used in the calculation of closure temperatures

Mineral	Sample	D_0 (cm ² s ⁻¹)	E (kcal mole ⁻¹)	Diffusion geometry	A	Data source
Muscovite	RR58C	0.000138	40	Cylinder	27	Robbins (1972)
Biotite						
(Fe ²⁺ = 0.495) ^a	RR58B	0.1012	47.96	Cylinder	27	Giletti (1974)
(Fe ²⁺ = 0.511) ^a	RR58C	0.0941	47.63	Cylinder	27	Harrison et al. (1985)

^a Fe²⁺ = Fe/(Fe + Mg): Since the argon diffusivity of biotite is controlled by its chemical composition, the diffusion data are calculated with using a regression of diffusion data for the biotites published in Giletti (1974) and Harrison et al. (1985).

same as those found by previous studies (Harrison et al., 1996; Wang et al., 1998).

6. Discussion and conclusions

As mentioned earlier, understanding of the time sequence of tectonic events is of significance in revealing the mechanism of extrusion tectonics and the opening of marginal seas in SE Asia. If the left-lateral shear movement along the ASRR shear

zone predated or occurred simultaneously to the opening of the South China Sea, the collision between the Eurasian and Indian plates possibly may have been responsible for shearing along the ASRR shear zone and the opening of the South China Sea, as suggested by the collision/extrusion model proposed by Tapponnier et al. (1982, 1986). In contrast, if the onset of the shear movement postdates the opening of the South China Sea, extrusion tectonics may not be the cause for the opening of the South China Sea, and the collision/

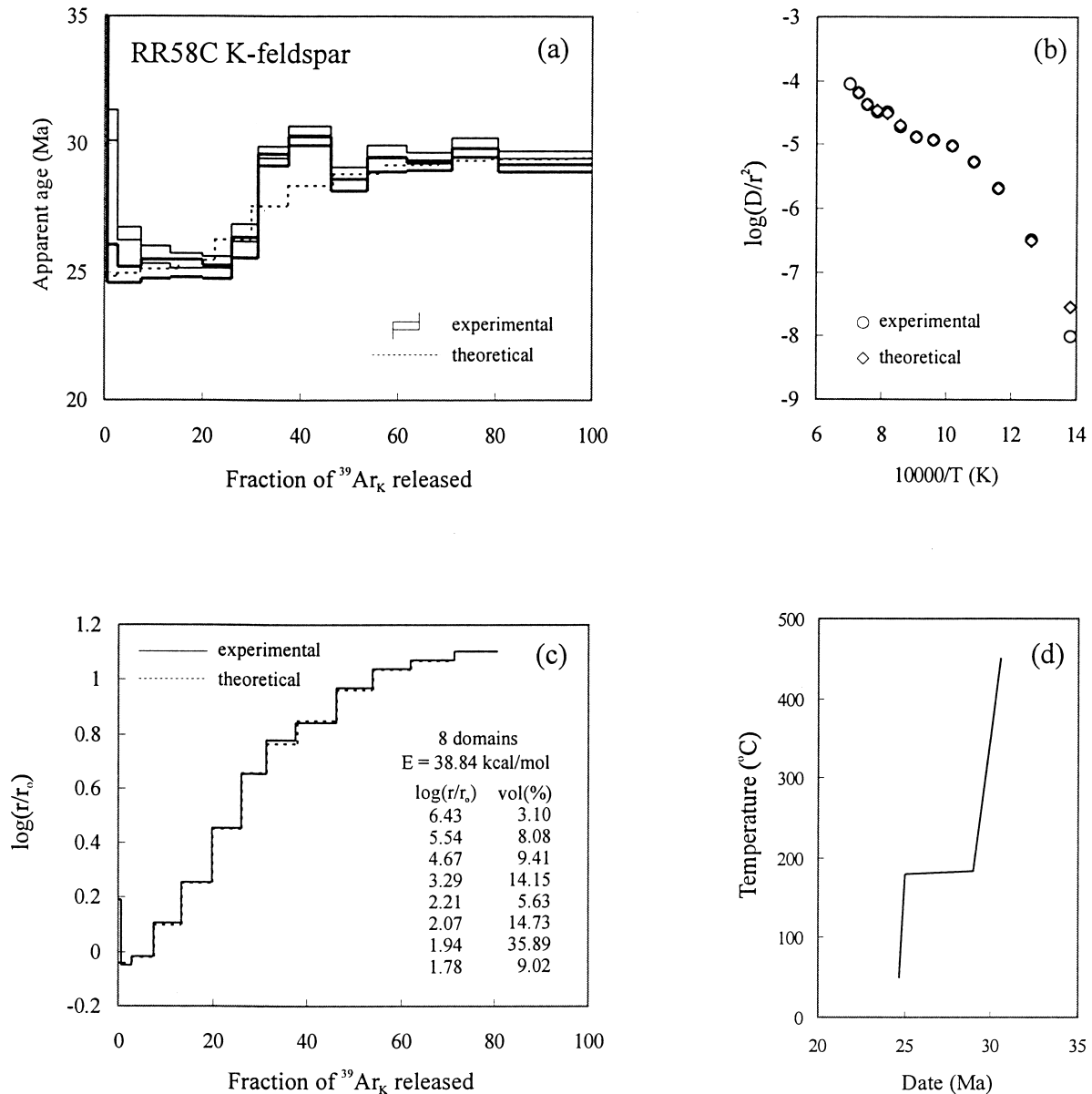


Fig. 4. (a) Experimental and theoretical age spectra for RR58C K-feldspar. The thin curve is the theoretical age spectrum using the diffusion parameter and cooling history shown in (b) through (d) assuming a single activation. (b) Arrhenius plot calculated from the experimental results assuming the plane slab diffusion geometry from measured $^{39}\text{Ar}_k$ loss during the step-heating experiment. (c) $\log(r/r_0)$ plot together with theoretical fit for single activation assumption. (d) Proposed cooling history that produces an excellent fit to the age spectrum in Fig. 4(a).

extrusion model may need further evaluation, as suggested by Chung et al. (1997) and Wang et al. (1998).

It is generally accepted that shearing along the ASRR Shear Zone has not only resulted in fast cooling of the metamorphic massifs, but also induced anatectic metamorphism of metamorphic rocks, resulting in the generation of leucogranites in the shear zone due to the high temperature associated with the shearing in the metamorphic massifs (Tapponnier et al., 1990; Leloup et al., 1995). Thus, chronological data for the igneous and metamorphic rocks in the ASRR Shear Zone would potentially provide most useful constraints for

revealing the timing of the movement along the shear zone.

Based on a U–Pb date (35.0 ± 0.1 Ma) for an alkaline intrusion close to, but outside the ASRR Shear Zone in SW Yunnan, Schärer et al. (1994) suggested that the sinistral movement along the ASRR Shear Zone might have started as early as 35 Ma. However, after systematically studying the Paleogene alkaline rocks cropping out in wide areas in eastern Tibet, SW China, and NW Vietnam, Chung et al. (1998, 1999) argued that these alkaline rocks actually have been generated by partial melting of thickened lithosphere mantle after the collision of India–Asian continents.

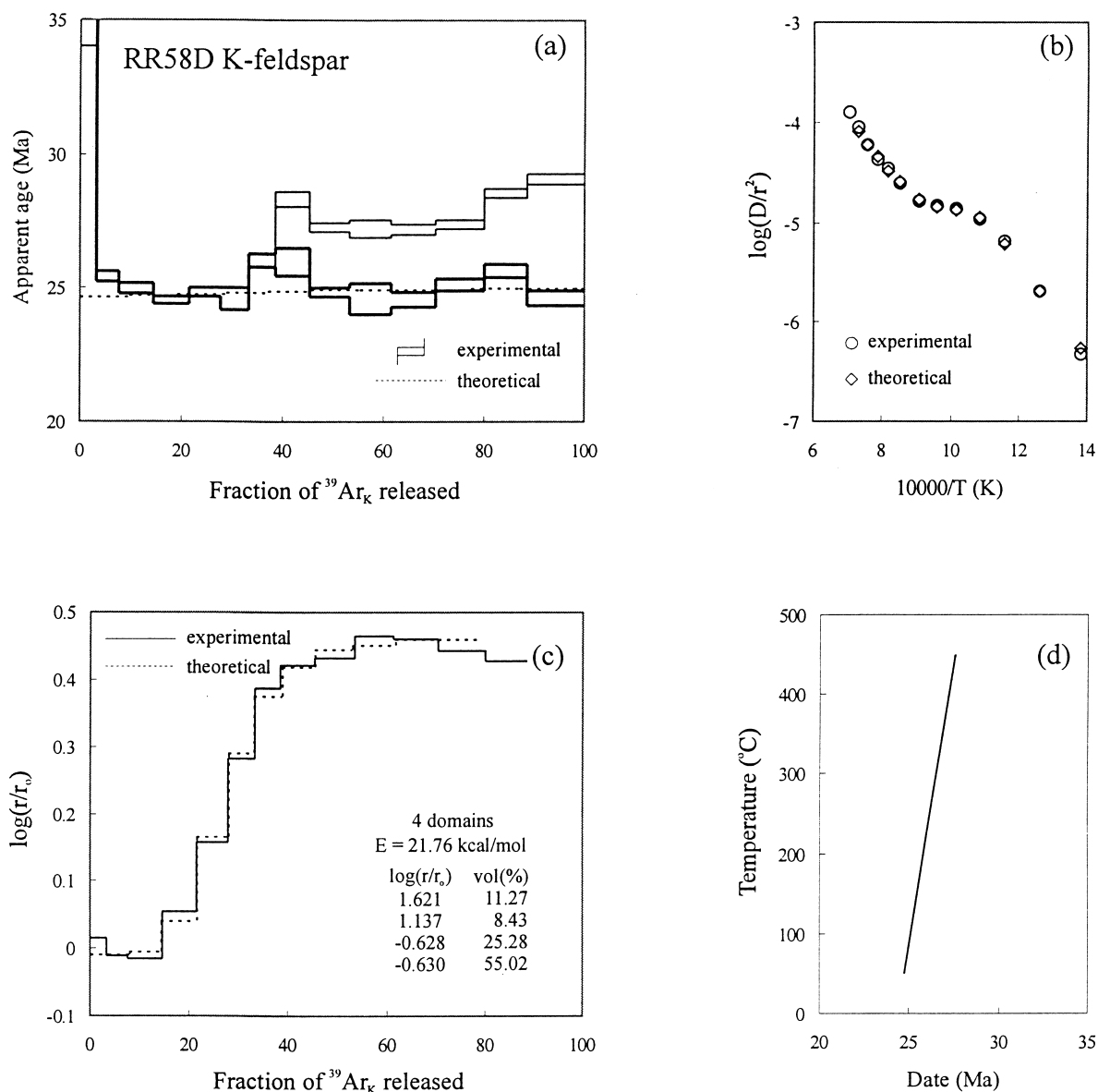


Fig. 5. (a) Age spectra, (b) Arrhenius plot, (c) $\log(r/r_0)$ plot, (d) modelled cooling history for RR58D K-feldspar. As shown in the $^{36}\text{Ar}/^{40}\text{Ar}$ - $r-^{39}\text{Ar}/^{40}\text{Ar}$ correlation diagram, apparent ages for high temperature steps were affected by excess argon with large $^{40}\text{Ar}/^{36}\text{Ar}$ value. After correcting the possible effect of excess argon, the ages of these steps are recalculated and plotted as hatched rectangles in the age spectra.

Their chemical characters preclude formation by partial melting of crustal rocks as a result of shear heating of the ASRR Shear Zone. Forty sets of high-quality $^{40}\text{Ar}/^{39}\text{Ar}$ and K–Ar dates for these Paleogene alkaline rocks suggested that the high-alkali magmatism occurred during the period of 40–30 Ma (Chung et al., 1998, 1999). On the basis of a good correlation of the Paleogene alkaline magmatic suites across the ASRR Shear Zone in SW China and northern Vietnam, Chung et al. (1997) further suggested that the left-lateral offset along the ASRR Shear Zone was younger than ~30 Ma. In other words, the wide occurrence of Paleogene alkaline magmatic activity does not favour the assumption of contemporaneous large amounts of strike-slip movement along the ASRR Shear Zone and the movement of the ASRR Shear Zone may not have started before ~30 Ma (Chung et al., 1997, 1998, 1999). Hence, chronological data for the Paleogene alkaline rocks in this region ranging from 35 to 22 Ma (Schärer et al., 1990, 1994; Tapponnier et al., 1990; Zhang and Schärer, 1999) may not be useful in precisely delineating the movement of the ASRR Shear Zone.

Alternatively, the movement of the ASRR Shear Zone may also potentially be constrained by thermochronological data for the metamorphic rocks in the shear zone, as the movement of major faults can potentially induce exhumation of metamorphic massifs and rapid cooling (Harrison et al., 1996; Wang et al.,

1998). In the past few years, the metamorphic massifs in the ASRR Shear Zone have been studied intensively by the $^{40}\text{Ar}/^{39}\text{Ar}$ thermochronological method (Leloup et al., 1993; Harrison et al., 1992, 1996; Wang et al., 1998). The results at hand show that the metamorphic rocks in the ASRR Shear Zone have experienced rapid cooling in the period of 27–17 Ma. They also indicate that the metamorphic massifs were exhumed diachronously from southeast to northwest along the shear zone, due to the northwestward propagation of trans-tensional deformation, at a rate in the range of 4–5 cm y^{-1} (Harrison et al., 1996; Wang et al., 1998). Therefore, chronological data from the southeasternmost part of the metamorphic massif, cropping out in the Nam Dinh area, NE Vietnam, would be one of the most helpful constraints for revealing the onset timing of the left-lateral movement of the ASRR Shear Zone.

As discussed in previous sections, the rocks from the Nam Dinh area started rapid cooling at ~27 Ma (Fig. 6) which appears to be slightly older than the age obtained by Wang et al. (1998) from the northwest part of the Day Nui Con Voi metamorphic massif in NW Vietnam. It is not too surprising to see such an older age record, because previous studies (Harrison et al., 1996; Wang et al., 1998) suggested that the exhumation of the metamorphic massifs appears to be diachronous, starting in the southeast and propagating northwest. However, the age of ~27 Ma may still not be considered as the best estimate for the onset of movement along the ASRR Shear Zone, because this sampling locality is still some distance from the boundary fault which is located close to the shoreline of east Vietnam. In order to estimate the onset timing of the left-lateral movement of the ASRR Shear Zone, a plot of the rapid cooling ages versus distances of the out-

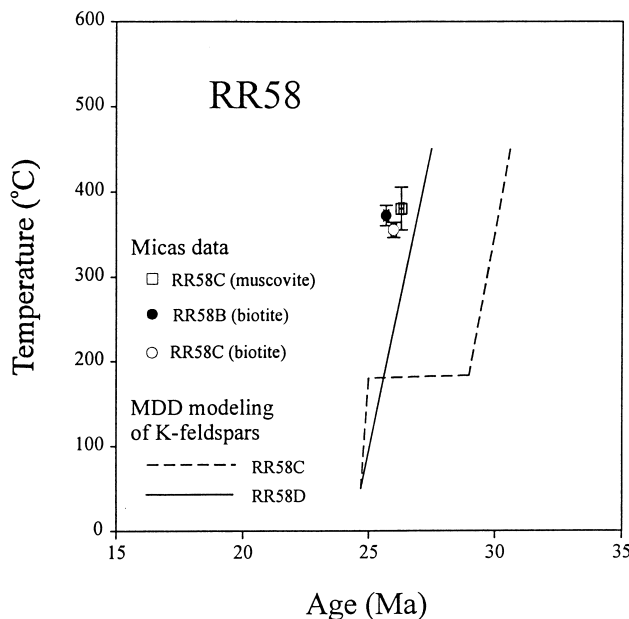


Fig. 6. Cooling paths for the samples. Closure temperatures for micas are calculated using suitable argon diffusion parameters and half of grain size as diffusion dimension. Cooling curves from K-feldspar $^{40}\text{Ar}/^{39}\text{Ar}$ analyses are obtained by applying the multiple-domain diffusion hypothesis shown in Figs. 4 and 5.

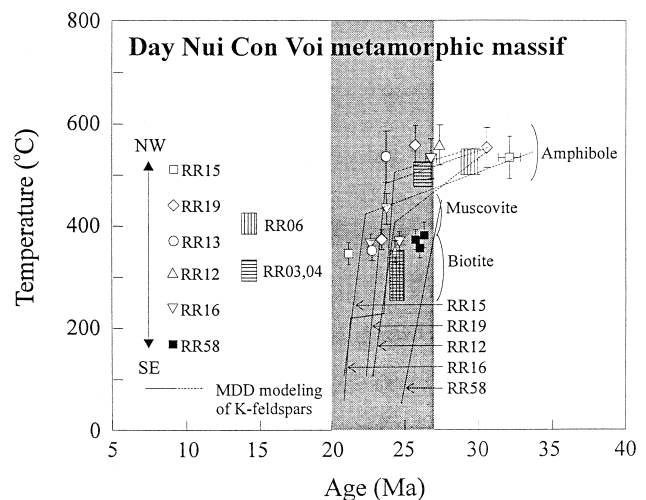


Fig. 7. Compilation of cooling paths for the metamorphic rocks in the Day Nui Con Voi metamorphic massif. Data sources: Nam et al. (1998), Wang et al. (1998), and the present study.

crops of metamorphic rocks away from the boundary fault along the shoreline of Indochina is presented in Fig. 8. If the left-lateral movement of the ASRR Shear Zone is truly propagating from southeast to northwest, the intercept of the linear younging trend of the rapid cooling ages would be the best estimate for the onset timing of the left-lateral shearing along the ASRR Shear Zone. From Fig. 8 it is evident that the Day Nui Con Voi metamorphic massif was exhumed diachronously from southeast to northwest at a rate of about 6 cm y^{-1} . The onset of shear movement along the ASRR Shear Zone at its southeastern end may have occurred at about 27.5 Ma. Such a conclusion is in perfect agreement with the results of previous thermochronological studies, showing that all metamorphic rocks in the ASRR Shear Zone were rapidly exhumed after 27.5 Ma (Leloup et al., 1993; Harrison et al., 1996; Wang et al., 1998; Nam et al., 1998).

The present results suggest that the movement along the ASRR Shear Zone started at around 27.5 Ma. A large-scale displacement along the ASRR Shear Zone before 29.1 Ma is not possible, because of a good correlation of Paleogene alkaline magmatic suites across the shear zone in SW China and NW Vietnam, with a youngest age of $29.1 \pm 0.8 \text{ Ma}$ (Chung et al., 1997). Therefore, it may be concluded that the left-lateral movements along the ASRR Shear Zone started at around 27.5 Ma. This implies that the initiation of the ASRR Shear Zone postdates the opening of the South China Sea, starting at around 30 Ma as inferred from the magnetic records in the South China Sea (Taylor

and Hayes, 1983; Briaies et al., 1993), calibrated with the newly published geomagnetic polarity timescale (Cande and Kent, 1995). Such a time sequence is totally different from that expected from the collision–extrusion model, as widely advocated by many previous authors (Tapponnier et al., 1982, 1986; Peltzer and Tapponnier, 1988; Briaies et al., 1993; Leloup et al., 1995). This would imply that shearing along the ASRR Shear Zone is not directly responsible for the opening of the South China Sea, hence the opening of the South China Sea should have been driven by other mechanisms.

Interestingly enough, a similar conclusion was reached by previous geophysical studies of the offshore area of Vietnam (Rangin et al., 1995; Roques et al., 1997). Rangin et al. (1995) studied seismic profiles of the Tonkin Gulf, and found that the left-lateral offset of the Red River Fault may not have exceeded a few tens of kilometers in the offshore area of Vietnam. This observation is totally different from the large-scale displacement of the ASRR Shear Zone inferred from the onshore data (see Leloup et al., 1995; Chung et al., 1997 for summary and discussion). They suspected that the fault system may have been partitioned into various fault systems or ceased in the offshore area (Rangin et al., 1995). Seismic and gravity data presented by Roques et al. (1997) show a dextral motion along the boundary fault, with an ambiguous relationship to the sinistral motion along the ASRR Shear Zone in the offshore area of Vietnam. All these offshore geophysical data seem to question models proposing a genetic linkage between the opening of the South China Sea and the left-lateral movement along the ASRR Shear Zone (Rangin et al., 1995; Roques et al., 1997). It thus appears that the geophysical data provide independent evidence supporting our conclusion that the left-lateral movement along the ASRR Shear Zone is not responsible for the opening of the South China sea.

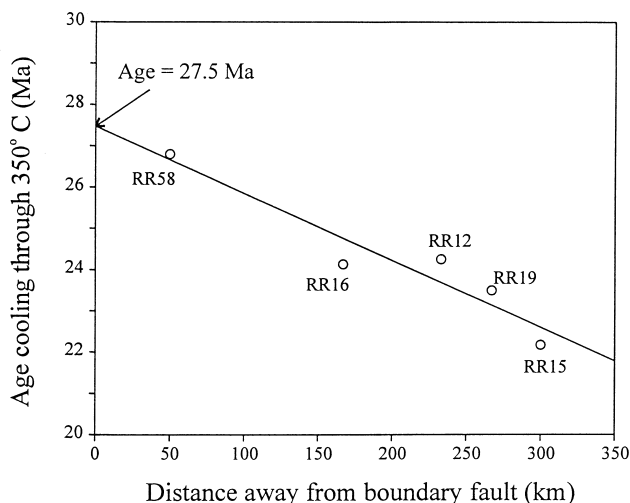


Fig. 8. Plot of the ages of rapid cooling versus sample location for samples in the Day Nui Con Voi massif. The age data were extracted from the cooling paths considering cooling below 350°C , shown in Fig. 7. The good correlation indicates the northwestward propagation of exhumation in response to the left-lateral shear movement along the ASRR zone. The intercept on the y -axis suggests the onset age of the left-lateral shearing of the ASRR zone to be about 27.5 Ma.

Acknowledgements

The authors are indebted to Drs Dinh Van Toan and Cung T. Chi of the National Center for Natural Sciences and Technology for their kind help with the field trip in Vietnam, Dr O.M. Lovera for kindly providing the program of multiple-domain diffusion modelling, and Dr G.S. Odin for providing a split of the LP-6 biotite standard. This paper has benefited from the constructive comments of Drs C. Rangin and U. Knittel. The present study is financially supported by a grant from the National Science Council (NSC-87-2116-M-002-020-Y), Taiwan.

References

- Briais, A., Patriat, P., Tapponnier, P., 1993. Updated interpretation of magnetic anomalies and seafloor spreading stages in the South China Sea: Implications for the Tertiary tectonics of Southeast Asia. *Journal of Geophysical Research* 98, 6299–6328.
- Cande, S.C., Kent, D.V., 1995. Revised calibration of the geomagnetic polarity timescale for the Late Cretaceous and Cenozoic. *Journal of Geophysical Research* 100, 6093–6095.
- Chung, S.-L., Lee, T.-Y., Lo, C.-H., Wang, P.-L., Chen, C.-Y., Yem, N.T., Hoa, T.T., Genyao, W., 1997. Intraplate extension prior to continental extrusion along the Ailao Shan–Red River Shear Zone. *Geology* 25, 311–314.
- Chung, S.-L., Lo, C.-H., Lee, T.-Y., Zhang, Y., Xie, Y., Li, X., Wang, K.-L., Wang, P.-L., 1998. Diachronous uplift of the Tibetan plateau starting from 40 Myr age. *Nature* 294, 769–773.
- Chung, S.-L., Wang, K.-L., Lo, C.-H., Lan, C.-Y., Zhang, Y., Xie, Y., Li, X., Lee, T.-Y., Thanh, H.H., Hoa, T.T., 1999. Age and origin of magmatism along the Cenozoic Red River shear belt, China: Discussion and new constraints from Vietnam. *Contributions to Mineralogy and Petrology* (submitted).
- Dodson, M.H., 1973. Closure temperature in cooling geochronological and petrological systems. *Contributions to Mineralogy and Petrology* 40, 259–274.
- Geological Survey of Vietnam 1988. Geologic map of Vietnam: Hanoi, Geological Survey of Vietnam, scale 1:500,000.
- Giletti, B.J., 1974. Studies in diffusion I: Ar in phlogopite mica. In: Hofmann, A.W., Giletti, B.J., Yoder, H.S., Yund, R.A. (Eds.), *Geochemical Transport and Kinetics*, Carnegie Institute Washington Publication 634, pp. 107–115.
- Harrison, T.M., Chen, W., Leloup, P.H., Ryerson, F.J., Tapponnier, P., 1992. An early Miocene transition in deformation regime within the Red River fault zone, Yunnan, and its significance for Indo-Asian tectonics. *Journal of Geophysical Research* 97, 7159–7182.
- Harrison, T.M., Duncan, I., McDougall, I., 1985. Diffusion of ^{40}Ar in biotite: Temperature, pressure and compositional effects. *Geochimica et Cosmochimica Acta* 49, 2461–2468.
- Harrison, T.M., Leloup, P.H., Ryerson, F.J., Tapponnier, P., Lacassin, R., Wenji, C., 1996. Diachronous initiation of transtension along the Ailao Shan–Red River Shear Zone, Yunnan and Vietnam. In: Yin, A., Harrison, T.M. (Eds.), *The Tectonic Evolution of Asia*. Cambridge University Press, pp. 205–226.
- Leloup, P.H., Harrison, M., Ryerson, F.J., Chen, W., Li, Q., Tapponnier, P., Lacassin, R., 1993. Structural, petrological and thermal evolution of a Tertiary strike-slip shear zone, Diancang Shan, Yunnan. *Journal of Geophysical Research* 98, 6715–6743.
- Leloup, P.H., Lacassin, R., Tapponnier, P., Schärer, U., Dalai, Z., Xiaohan, L., Liangshang, Z., Shaocheng, J., Trinh, P.T., 1995. The Ailao Shan–Red River Shear Zone (Yunnan, China), Tertiary transform boundary of Indochina. *Tectonophysics* 251, 3–84.
- Lo, C.-H., Lee, C.-Y., 1994. $^{40}\text{Ar}/^{39}\text{Ar}$ method of K–Ar age determination of geological samples using the Tsing-Hua Open-Pool Reactor (THOR). *Journal of the Geological Society of China* 37, 143–164.
- Lovera, O.M., Richter, F.M., Harrison, T.M., 1991. Diffusion domains determined by ^{39}Ar released during step heating. *Journal of Geophysical Research* 96, 2057–2069.
- McDougall, I., Harrison, T.M., 1988. *Geochronology and Thermochronology by the $^{40}\text{Ar}/^{39}\text{Ar}$ Method*. Oxford University Press, 215 pp.
- Nam, T.N., Toriumi, M., Itaya, T., 1998. P-T-t paths and post-metamorphic exhumation of the Day Nui Con Voi Shear Zone in Vietnam. *Tectonophysics* 290, 299–318.
- Odin, G.S., 35 collaborators, 1982. Interlaboratory standards for dating purposes. In: Odin, G.S. (Ed.), *Numerical Dating in Stratigraphy*. Wiley, pp. 123–149.
- Peltzer, G., Tapponnier, P., 1988. Formation and evolution of strike-slip faults, rifts, and basins during the India–Asia collision. An experimental approach. *Journal of Geophysical Research* 93, 15085–15117.
- Rangin, C., Klein, M., Roques, D., Le Pichon, X., Trong, L.V., 1995. The Red River fault system in the Tonkin Gulf, Vietnam. *Tectonophysics* 243, 209–222.
- Robbins, G.A. 1972. Radiogenic argon diffusion in muscovite under hydrothermal conditions. MSc Thesis, Brown University.
- Roques, D., Matthews, S.J., Rangin, C., 1997. Constraints on strike-slip motion from seismic and gravity data along the Vietnam margin offshore Da Nang: Implications for hydrocarbon prospectivity and opening of the East Vietnam Sea. In: Fraser, A.J., Matthews, S.J., Murphy, R.W. (Eds.), *Petroleum Geology of Southeast Asia*, Geological Society of London Special Publication 125, pp. 341–353.
- Schärer, U., Tapponnier, P., Lacassin, R., Leloup, P.H., Zhong, D., Ji, S., 1990. Intraplate tectonics in Asia: A precise age for large-scale Miocene movement along the Ailao Shan–Red River Shear Zone, China. *Earth and Planetary Science Letters* 97, 65–77.
- Schärer, U., Zhang, L.-C., Tapponnier, P., 1994. Duration of strike-slip movements in a large shear zone: the Red River belt, China. *Earth and Planetary Science Letters* 126, 379–397.
- Tapponnier, P., Lacassin, R., Leloup, P.H., Schärer, U., Zhou, D., Wu, H., Liu, X., Ji, S., Zhang, L., Zhong, J., 1990. The Ailao Shan/Red River metamorphic belt: Tertiary left-lateral shear between Indochina and South China. *Nature* 343, 431–437.
- Tapponnier, P., Peltzer, G., Armijo, R., 1986. On the mechanics of the collision between India and Asia. In: Coward, M.P., Ries, A.C. (Eds.), *Collision Tectonics*, Geological Society of London Special Publication 19, pp. 115–157.
- Tapponnier, P., Peltzer, G., Armijo, R., Le Dain, A.-Y., Cobbold, P., 1982. Propagating extrusion tectonics in Asia: New insights from simple experiments with plasticine. *Geology* 10, 611–616.
- Taylor, B., Hayes, D.E., 1983. Origin and history of the South China Sea. In: Hayes, D.E. (Ed.), *Tectonic and Geologic Evolution of Southeast Asian Seas and Islands, Part 2*, American Geophysical Union Monograph 27, pp. 23–56.
- Wang, P.-L., Lo, C.-H., Lee, T.-Y., Chung, S.-L., Lan, C.-Y., Yem, N.T., 1998. Thermochronological evidence for the movement of the Ailao Shan–Red River Shear Zone: A perspective from Vietnam. *Geology* 26, 887–890.
- Zhang, L.-S., Schärer, U., 1999. Age and origin of magmatism along the Cenozoic Red River shear belt, China. *Contributions to Mineralogy and Petrology* 134, 67–85.